Damping of linear spin-wave modes in magnetic nanostructures: Local, nonlocal, and coordinate-dependent damping

Roman Verba*
Institute of Magnetism, Kyiv 03680, Ukraine

Vasil Tiberkevich and Andrei Slavin
Department of Physics, Oakland University, Rochester, Michigan 48309, USA

(Received 29 May 2018; published 6 September 2018)

A general perturbation theory for the description of weak damping of linear spin-wave modes in magnetic nanostructures is developed. This perturbative approach allows one to account for the usual uniform Gilbert damping, as well as for the spatially nonuniform (coordinate-dependent) and nonlocal (magnetization-texture-dependent) Gilbert-like dissipation mechanisms. Using the derived general expression, it is possible to calculate the damping rate of a particular spin-wave mode if the frequency and the spatial profile of this mode, along with the relevant parameters of a magnetic material, are known. The examples demonstrating the applications of the developed general formalism include (i) generalization of the damping rate of a spin-wave mode propagating in a magnetic sample for the case of a nonuniform static magnetization or/and bias magnetic field, (ii) calculation of a damping rate of a gyrotropic mode in a vortex-state magnetic nanodot, (iii) evaluation of the spin diffusion influence on the damping rate of spin-wave modes in a conducting ferromagnet, and (iv) calculation of damping rates of spin-wave modes in a ferromagnetic film in the presence of a spin pumping into an adjacent nonmagnetic metal layer. The developed formalism is especially useful in micromagnetic simulations, as it allows one to calculate damping rates of spin-wave modes based on the numerical solution of a conservative eigenmode problem.

DOI: 10.1103/PhysRevB.98.104408

I. INTRODUCTION

Understanding the mechanisms of magnetic damping and ability to calculate damping rates for magnetic eigenexcitations—spin-wave (SW) modes—is critically important for the applications of magnetic materials in data storage, information processing, and microwave technologies. In particular, the SW damping rate determines such important characteristics as the time of the magnetization reversal of a magnetic memory element (in precessional regime) [1], the linewidth of a ferromagnetic resonance [2], the threshold current in spin-torque devices [3], etc. A rigorous consideration of a magnetic damping, even in bulk ferromagnetics, is very complicated, since there are many different mechanisms of energy dissipation, such as magnon-electron and magnon-phonon scattering. Also multimagnon processes could contribute to the damping rate of some SW modes [2,4].

Instead of a rigorous consideration, magnetic damping is, usually, taken into account phenomenologically using the Gilbert model [5], within which the dissipative torque, acting on magnetization, is proportional to the time derivative of magnetization and the Gilbert damping parameter α_G. The damping rate of a SW mode is then given by $\Gamma_\nu = \alpha_G \epsilon_\nu \omega_\nu$, where ω_ν is the mode frequency and the coefficient ϵ_ν describes the effect of the magnetization precession ellipticity. Analytical expressions for ϵ_ν were derived in many important particular cases, e.g., for spin waves propagating in a uniformly magnetized ferromagnetic film [6], for the gyrotropic mode of magnetic vortex [7], etc. The Gilbert model describes the magnetic damping in bulk ferromagnetic samples reasonably well within several limitations, in particular, when the damping rate is relatively small, and the magnitude of the dynamic magnetization is also not large. Recently, the Gilbert model of magnetic dissipation was also generalized to the case of a substantially nonlinear magnetization dynamics [8].

In thin ferromagnetic films and magnetic nanostructures, in addition to the bulk uniform damping, other damping mechanisms, such as spatially nonuniform (coordinate dependent) or nonlocal (dependent on the magnetization texture) damping could be present. These additional damping mechanisms include the spin pumping from a ferromagnetic layer into an adjacent normal metal layer [9,10], longitudinal and transverse spin diffusion [11–13], chiral damping [14], and spin-wave scattering on technological imperfections [15,16] (edge damage). In many cases, these coordinate-dependent and magnetization-texture-dependent damping mechanisms could be of the same order of magnitude or stronger than the traditional uniform Gilbert damping, and, also, could create different contribution to the SW modes having different spatial profiles [17–19]. Naturally, these mechanisms cannot be taken into account by a simple renormalization of a Gilbert damping constant α_G, same for all the SW modes.

In several particular cases, the influence of the interlayer spin pumping and transverse spin diffusion on the damping rate of SW modes with different spatial profiles has been

*corresponding author: verrv@ukr.net

already discussed [18–26]. In this paper, we present a general formalism, which allows one to calculate the SW mode damping rate in the presence of the uniform Gilbert damping, as well as the coordinate-dependent and magnetization-texture-dependent damping mechanisms. As shown below, when the damping rate is relatively small, it can be calculated, provided one knows the SW mode frequency and spatial profile, obtained in the *conservative* approach. It is especially important since for many practically important cases the problem of calculation of the SW mode profile has been already solved. In many cases, the SW mode profile can be obtained numerically using various powerful and general micromagnetic codes [27,28]. In contrast, accurate micromagnetic simulations of *dissipative* processes require much more simulation time. Also, common micromagnetic codes, typically, can take into account only the standard uniform Gilbert damping, while accounting for the additional dissipation mechanisms requires a substantial modification and a subsequent verification of the micromagnetic code.

The paper has the following structure. In Sec. II, following Refs. [29–31], we review the elements of the general theory of linear SW excitation in magnetic structures. Using this theory, a general expression for the SW mode damping rate under the influence of a linear magnetic damping is derived in Sec. III. Then, we present examples of application of the developed formalism, showing how its results are related to the previous results obtained in several known particular cases, as well as demonstrating some new results. In Sec. IV, we consider the SW damping caused by a uniform Gilbert damping in magnetic samples with nonuniform static magnetization, in particular, in vortex-state magnetic dots. The effects of additional dissipation mechanisms, such as spin diffusion and interlayer spin pumping, are considered in Secs. V and VI, respectively. Finally, conclusions are given in Sec. VII.

II. PRINCIPAL EQUATIONS

Let us consider the magnetization dynamics of a finite-size ferromagnetic sample, e.g., film, nanodot, etc. The conservative dynamics of a magnetization vector $\boldsymbol{M} = \boldsymbol{M}(\boldsymbol{r}, t)$ in such a case is described by the Landau-Lifshitz equation

$$\frac{\partial \boldsymbol{M}(\boldsymbol{r}, t)}{\partial t} = \gamma(\boldsymbol{B}_{\text{eff}} \times \boldsymbol{M}(\boldsymbol{r}, t)) , \tag{2.1}$$

where γ is the modulus of the gyromagnetic ratio and $\boldsymbol{B}_{\text{eff}} = \boldsymbol{B}_e - \mu_0 \hat{\boldsymbol{G}} * \boldsymbol{M}$ is the effective magnetic field. Here, $\boldsymbol{B}_e$ is an external magnetic field and the self-adjoint tensor operator $\hat{\boldsymbol{G}}$ describes the magnetic self-interaction: nonuniform exchange, magnetodipolar interaction, and magnetic anisotropy (explicit expression for $\hat{\boldsymbol{G}}$ could be found, e.g., in Refs. [29,31]).

Considering *linear* dynamical processes one can represent the magnetization vector as $\boldsymbol{M}(\boldsymbol{r}, t) = M_s[\boldsymbol{\mu}(\boldsymbol{r}) + \boldsymbol{m}(\boldsymbol{r}, t)]$, where M_s is the saturation magnetization, the unit vector $\boldsymbol{\mu}$ describes the static magnetic configuration of the ferromagnetic sample, and the dimensionless vector $\boldsymbol{m}$ describes the small deviation from the static configuration. Using this representation in Eq. (2.1) one can, finally, obtain the following equation for frequencies ω_ν and profiles $\boldsymbol{m}_\nu$ of the SW eigenmodes of a ferromagnetic body:

$$-i\omega_\nu \boldsymbol{m}_\nu = \boldsymbol{\mu} \times \hat{\boldsymbol{\Omega}} * \boldsymbol{m}_\nu , \tag{2.2}$$

where $\hat{\boldsymbol{\Omega}}$ is the Hamiltonian operator defined by the expression $\hat{\boldsymbol{\Omega}} = \gamma B \hat{\boldsymbol{I}} + \gamma \mu_0 M_s \hat{\boldsymbol{G}}$, B is the modulus of the static effective field, and $\hat{\boldsymbol{I}}$ is the identity matrix. In the same manner, one can, also, consider the propagating spin waves (e.g., in a ferromagnetic film), which are characterized by their wave vector $\boldsymbol{k}$. The only change in this case appears in the definition of the Hamiltonian operator, which should be defined as $\hat{\boldsymbol{\Omega}}_{\boldsymbol{k}} = \gamma B \hat{\boldsymbol{I}} + \gamma \mu_0 M_s e^{-i\boldsymbol{k}\cdot\boldsymbol{r}}(\hat{\boldsymbol{G}} * e^{i\boldsymbol{k}\cdot\boldsymbol{r}})$. Naturally, the Hamiltonian operators $\hat{\boldsymbol{\Omega}}$ and $\hat{\boldsymbol{\Omega}}_{\boldsymbol{k}}$ are also self-adjoint. Using this property, one can show that different SW modes of a ferromagnetic body satisfy the following orthogonality relation:

$$\langle \boldsymbol{m}^*_{\nu'} \cdot \boldsymbol{\mu} \times \boldsymbol{m}_\nu \rangle = -i A_\nu \delta_{\nu,\nu'} , \tag{2.3}$$

where index ν is used to enumerate the SW modes, symbols $\langle \dots \rangle$ denote averaging over all the volume of the ferromagnetic material, and A_ν is a real normalization constant of an SW eigenmode.

The influence of various small effects on the magnetization dynamics can be effectively considered in the framework of a perturbation theory. In a general case, accounting for a perturbation leads to the change of the effective field in Eq. (2.1) as $\boldsymbol{B}_{\text{eff}} \to \boldsymbol{B}_{\text{eff}} + \boldsymbol{b}$, where $\boldsymbol{b}(\boldsymbol{r})$ is an effective perturbation field, which could depend on time or/and on the magnetization $\boldsymbol{M}$. Considering only the processes that are linear in SW mode amplitudes, one can represent the dynamic magnetization as an infinite series in SW eigenmodes. Using this representation in the perturbed Landau-Lifshitz equation, one can obtain the following dynamical equation for the SW eigenmode amplitudes $c_\nu(t)$:

$$\frac{dc_\nu}{dt} = -i\omega_\nu c_\nu + i\gamma b_\nu - i\gamma \sum_{\nu'} (S_{\nu,\nu'} c_{\nu'} + \tilde{S}_{\nu,\nu'} c^*_{\nu'}) . \tag{2.4}$$

Here, the summation goes only over modes with positive norms, $A_{\nu'} > 0$ (see details in Ref. [30]) and the coefficients are equal to

$$b_\nu = \frac{1}{A_\nu} \langle \boldsymbol{m}^*_\nu \cdot \boldsymbol{b} \rangle, \tag{2.5a}$$

$$S_{\nu,\nu'} = \frac{1}{A_\nu} \langle (\boldsymbol{m}^*_\nu \cdot \boldsymbol{m}_{\nu'})(\boldsymbol{\mu} \cdot \boldsymbol{b}) \rangle, \tag{2.5b}$$

$$\tilde{S}_{\nu,\nu'} = \frac{1}{A_\nu} \langle (\boldsymbol{m}^*_\nu \cdot \boldsymbol{m}^*_{\nu'})(\boldsymbol{\mu} \cdot \boldsymbol{b}) \rangle . \tag{2.5c}$$

The above derived equations allow one to effectively describe the excitation of SW modes by an external microwave field, parametric processes under the parallel pumping, thermal fluctuations, etc., and, as it will be shown below, also describe the damping of the SW eigenmodes.

III. GENERAL PERTURBATION FORMALISM FOR THE LINEAR SPIN-WAVE DAMPING

In the framework of a Gilbert model, magnetic damping is taken into account phenomenologically by an additional term in the right-hand side of the Landau-Lifshitz equation

Eq. (2.1):

$$\boldsymbol{T}_G = \frac{\alpha_G}{M_s}\left(\boldsymbol{M} \times \frac{\partial \boldsymbol{M}}{\partial t}\right). \tag{3.1}$$

Many other dissipation mechanisms could be introduced by a similar, Gilbert-like term,

$$\boldsymbol{T}_{ad} = \frac{1}{M_s}\left(\boldsymbol{M} \times \left(\hat{\boldsymbol{D}}_{ad} * \frac{\partial \boldsymbol{M}}{\partial t}\right)\right). \tag{3.2}$$

Here, $\hat{\boldsymbol{D}}_{ad}$ is, in general, a tensor operator which could depend both on the spatial coordinate $\boldsymbol{r}$ and on the magnetization $\boldsymbol{M}$, but for the most common *linear* damping mechanisms it should not depend on the time derivative of the magnetization $\partial \boldsymbol{M}/\partial t$, since $\partial \boldsymbol{M}/\partial t$ is proportional to the SW amplitude. Note that for the dynamics of a constant-length magnetization vector $\boldsymbol{M}$, $|\boldsymbol{M}| = M_s$, only the component of the torque $\boldsymbol{T}_{ad}$ that is parallel to the vector $(\boldsymbol{M} \times \partial \boldsymbol{M}/\partial t)$ corresponds to the change of a magnetic energy, and, therefore, is responsible for the magnetic dissipation [4,8]. The other torque component, which is parallel to $(\partial \boldsymbol{M}/\partial t)$, affects the conservative magnetization dynamics, i.e., makes a contribution to the SW mode eigenfrequencies. Thus the effects that are described by Eq. (3.2), in general, could lead both to a change of the SW mode damping rate and to the change of its eigenfrequency.

Using the additional torque term in the form (3.2) one can take into account various dissipation mechanisms. In general, Eq. (3.2) could describe any mechanism of the intrinsic magnetic energy dissipation of a "liquid friction" type, which are, typically, the most important linear intrinsic damping mechanisms in bulk ferromagnets and ferromagnetic nanostructures. Below we consider in detail the influence of the spin diffusion and interlayer spin pumping (see Secs. V and VI) on the resultant dissipation rate of an SW mode. Also, using the formalism, presented below, one can easily consider additional damping in ferromagnets and their structures having large Rashba spin-orbit coupling. In this case, the dissipative torque has exactly the structure (3.2) with the damping tensor dependent on the static magnetization configuration (see explicit expression in Ref. [32]). Another important dissipation mechanism is the dynamic feedback in the ferromagnet–spin-Hall-metal heterostructures [33]. The corresponding dissipative torque in this case has linear and nonlinear terms; the last one, naturally, is important only for large-amplitude dynamics. The linear term can be also derived in the form of Eq. (3.2) with the damping tensor $\hat{\boldsymbol{D}}_{\rm fb} = \alpha_{\rm fb}\boldsymbol{e}_{z'} \otimes \boldsymbol{e}_{z'}$, where $\otimes$ denotes dyadic product of vectors, axis z' is directed perpendicularly to the ferromagnetic-normal metal interface and the coefficient $\alpha_{\rm fb}$ determines the efficiency of the dynamic feedback (see explicit expression in Ref. [33]).

The extrinsic mechanisms of energy pumping or dissipation, like a spin-torque produced by an external spin-polarized current (or a pure spin current) are described by a different term in the equation of motion [3,34,35]. This term is not proportional to the derivative $\partial \boldsymbol{M}/\partial t$, but, it could also be taken into account by a formalism similar to the one presented below.

Thus, as it follows from Eqs. (3.1) and (3.2), the effects of the common Gilbert damping and additional Gilbert-like damping mechanisms are described by the following effective field:

$$\boldsymbol{b} = \frac{1}{\gamma M_s}\hat{\boldsymbol{D}} * \frac{\partial \boldsymbol{M}}{\partial t}, \tag{3.3}$$

where $\hat{\boldsymbol{D}} = \alpha_G \hat{\boldsymbol{I}} + \hat{\boldsymbol{D}}_{ad}$. If the damping is relatively weak (i.e., if the damping rate of an SW mode is much smaller than the mode eigenfrequency), it can be considered using a perturbation theory.

In the above presented expression, we can use the zero-order approximation for the time derivative in the form

$$\partial \boldsymbol{M}/\partial t = M_s \sum_\nu \left[-i\omega_\nu c_\nu \boldsymbol{m}_\nu + \text{c.c.}\right], \tag{3.4}$$

which allows us to calculate explicitly the coefficients (2.5). The terms $S_{\nu\nu'}c_{\nu'}$ and $\tilde{S}_{\nu\nu'}c^*_{\nu'}$ in Eq. (2.4) correspond to three-magnon nonlinear interaction processes. These terms are of the second order of magnitude with respect to the SW amplitudes c_ν, and, thus, can be safely ignored in the consideration of the linear (small-amplitude) spin-wave dynamics. Finally, one gets the following equation describing the dynamics of the SW modes:

$$\frac{dc_\nu}{dt} = -i\omega_\nu c_\nu - \sum_{\nu'}\left(\Gamma_{\nu,\nu'}c_{\nu'} + \tilde{\Gamma}_{\nu,\nu'}c^*_{\nu'}\right), \tag{3.5}$$

where the coefficients are equal to

$$\Gamma_{\nu,\nu'} = \frac{\omega_{\nu'}}{A_\nu}\langle \boldsymbol{m}^*_\nu \cdot \hat{\boldsymbol{D}} * \boldsymbol{m}_{\nu'}\rangle, \quad \tilde{\Gamma}_{\nu,\nu'} = -\frac{\omega_{\nu'}}{A_\nu}\langle \boldsymbol{m}^*_\nu \cdot \hat{\boldsymbol{D}} * \boldsymbol{m}^*_{\nu'}\rangle. \tag{3.6}$$

It is clear, that the accounting for the magnetic dissipation leads to an additional dissipative coupling between the different SW modes, which results in a variation of the damping rates, mode profiles, and, to a smaller degree, the eigenfrequencies of the coupled modes in comparison with the case of zero intermode coupling. However, typically, the mode damping rates are small compared to the frequency difference between the neighboring SW eigenfrequencies, and one can safely ignore this damping-related coupling. In such a case, one obtains a standard equation for a damped oscillator, $dc_\nu/dt = -i\omega_\nu c_\nu - \Gamma_\nu c_\nu$, where the damping rate is defined as

$$\Gamma_\nu \equiv \Gamma_{\nu,\nu} = \frac{\omega_\nu}{A_\nu}\langle \boldsymbol{m}^*_\nu \cdot \hat{\boldsymbol{D}} * \boldsymbol{m}_\nu\rangle. \tag{3.7}$$

The damping-related coupling of the SW eigenmodes should be explicitly taken into account only near the points of SW mode degeneracy.

It follows from Eq. (3.7), that the common Gilbert damping in a ferromagnetic material could be described by the following expression for the SW mode damping rate:

$$\Gamma_\nu = \alpha_G \epsilon_\nu \omega_\nu, \tag{3.8}$$

where

$$\epsilon_\nu = \frac{\langle |\boldsymbol{m}_\nu|^2\rangle}{A_\nu}. \tag{3.9}$$

The properties of the "ellipticity" coefficient ϵ_ν are discussed below. If one assumes that the Gilbert dissipation parameter is coordinate-dependent, $\alpha_G = \alpha_G(\boldsymbol{r})$, the SW mode damping

rate is defined as $\Gamma_\nu = \omega_\nu \langle \alpha_G |\boldsymbol{m}_\nu|^2\rangle / A_\nu$. Such dependence takes place, for instance, near the boundaries of magnetic elements due to the technological imperfections [16,18]. Naturally, in such a case, the imperfections strongly affect the dissipation of the SW modes, which have greater oscillation power $|\boldsymbol{m}_\nu|^2$ in the spatial regions where the effective damping constant α_G is increased.

Representing the total damping rate of an SW mode, caused by different mechanisms, as

$$\Gamma_\nu = (\alpha_G + \Delta\alpha_{G,\nu})\epsilon_\nu \omega_\nu \,, \tag{3.10}$$

we arrive to the following expression for the effective enhancement of the Gilbert damping parameter, caused by additional dissipation mechanisms:

$$\Delta\alpha_{G,\nu} = \frac{\langle \boldsymbol{m}_\nu^* \cdot \hat{\boldsymbol{D}}_{ad} * \boldsymbol{m}_\nu \rangle}{\langle |\boldsymbol{m}_\nu|^2 \rangle} \,. \tag{3.11}$$

Obviously, the enhanced damping parameter affects differently the SW modes having a different spatial profiles, but this enhanced parameter does not depend directly on the SW mode eigenfrequency.

IV. EVALUATION OF A GILBERT DAMPING FOR SPIN-WAVE MODES

A. Relation of a Gilbert damping rate to the precession ellipticity and parameters of the spin-wave dispersion

As we have already pointed out, the damping rate of an SW mode, caused by common Gilbert damping, is determined by the mode structure via the coefficient ϵ_ν [Eq. (3.8)]. In the case of a spatially uniform magnetization precession, this coefficient can be directly related to the precession ellipticity:

$$\epsilon = 1 + \frac{\mathcal{E}^2}{2(1-\mathcal{E})} \,, \tag{4.1}$$

where $\mathcal{E} = 1 - m_{\min}/m_{\max}$ is the commonly used definition for the precession ellipticity [2]. It is clear that for circularly polarized magnetization precession, when $\mathcal{E} = 0$, the coefficient $\epsilon = 1$. When the magnetization precession becomes elliptically polarized, the value ϵ increases, and the damping rate becomes larger than $\alpha_G \omega_\nu$. This property of the SW mode damping is well-known in literature (see, e.g., Ref. [2]).

The value of the coefficient ϵ_ν can be, also, related to the dispersion relation of a particular SW mode. As it was shown by D. Stancil [6], in the case of SWs, propagating in a ferromagnetic film having *uniform* static magnetization at an arbitrary angle to the film plane, the coefficient ϵ_ν can be expressed as

$$\epsilon_\nu = \frac{\partial \omega_\nu}{\partial \omega_H} \,, \tag{4.2}$$

where ω_ν is the SW mode dispersion relation, and $\omega_H = \gamma B$, where B is the static internal magnetic field. The relation of the damping rate to the derivative $\partial\omega_\nu/\partial\omega_H$ becomes clear if one notes that for a uniform static magnetization, accounting of the Gilbert damping leads to only one modification in the linearized equation of motion, $\omega_H \to \omega_H + i\alpha_G\omega$ (see Eq. (1.68) in Ref. [2]). For the cases of the in-plane or perpendicular static magnetization of a film, expression (4.2) is simplified since $\partial\omega_\nu/\partial\omega_H = \gamma^{-1}\partial\omega_\nu/\partial B_e$, where B_e is the external magnetic field. This derivative can be easily calculated form the experimental data, and, therefore, can be used for the characterization of the SW modes and their damping rates.

Here we show that a relation similar to Eq. (4.2) can be derived in a general case when the static magnetization and the internal bias magnetic field of a magnetic sample can be coordinate-dependent. For this purpose, we take a variational derivative of both sides of Eq. (2.2) over some variable ξ. A straightforward calculation results in the following equation:

$$-(i\omega_\nu + \boldsymbol{\mu}\times\hat{\boldsymbol{\Omega}}) * \frac{\delta \boldsymbol{m}_\nu}{\delta\xi} = \left(i\frac{\delta\omega_\nu}{\delta\xi} + \boldsymbol{\mu}\times\frac{\delta\hat{\boldsymbol{\Omega}}}{\delta\xi} + \frac{\delta\boldsymbol{\mu}}{\delta\xi}\times\hat{\boldsymbol{\Omega}} \right) * \boldsymbol{m} \,. \tag{4.3}$$

Then, multiplying the above equation by $(\boldsymbol{m}_\nu^* \cdot \boldsymbol{\mu}\times)$, averaging the resulting equation over the volume of a magnetic sample, and taking into account the self-adjoint property of the operator $\hat{\boldsymbol{\Omega}}$, one can derive the following relation:

$$A_\nu \frac{\delta\omega_\nu}{\delta\xi} = -\left\langle \boldsymbol{m}_\nu^* \cdot \boldsymbol{\mu} \times \left(\boldsymbol{\mu}\times\frac{\delta\hat{\boldsymbol{\Omega}}}{\delta\xi} + \frac{\delta\boldsymbol{\mu}}{\delta\xi}\times\hat{\boldsymbol{\Omega}} \right) * \boldsymbol{m}_\nu \right\rangle . \tag{4.4}$$

Then, assuming that the static magnetization configuration of the sample is fixed, choosing the variable ξ as $\xi = \omega_H(\boldsymbol{r}) = \gamma B(\boldsymbol{r})$, and using the equality $\delta\hat{\boldsymbol{\Omega}}/\delta\omega_H = \hat{\boldsymbol{I}}$, we get the final expression for the "ellipticity" coefficient in the form

$$\epsilon_\nu = \frac{\langle |\boldsymbol{m}_\nu|^2 \rangle}{A_\nu} = \frac{\delta\omega_\nu}{\delta\omega_H} \,. \tag{4.5}$$

This expression is a generalization of Eq. (4.2) to the case of a nonuniform static magnetization and/or nonuniform static internal field in a magnetic sample. In the case when the static internal field is uniform, $\omega_H \notin f(\boldsymbol{r})$, Eq. (4.5) is reduced to Eq. (4.2), since the variational derivative is reduced to a simple partial derivative. The derived expression (4.4) is analogous to a well-known expression for a derivative of eigenvalues of a matrix [36], in which the vector $(\boldsymbol{m}_\nu^* \times \boldsymbol{\mu})$ has the meaning of a left-hand-side eigenvector.

B. Example: damping rate of gyrotropic mode of magnetic vortex

As an example of application of the above presented formalism, below we consider the damping of a gyrotropic mode in a vortex-state magnetic dot. The magnetization ground state in the form of a vortex is one of the simplest spatially nonuniform and topologically nontrivial magnetization configurations of a magnetic nanodot. It is characterized by a curling in-plane magnetization with a small out-of-plane core in the dot center (see inset in Fig. 1). The static magnetization distribution of a circular magnetic nanodot in a vortex state is given by

$$\boldsymbol{\mu}(\boldsymbol{r}) = p\cos\theta(r)\boldsymbol{e}_z + \chi\sin\theta(r)\boldsymbol{e}_\phi \,, \tag{4.6}$$

where p and χ are the vortex polarity and chirality, respectively. Here, we use the polar coordinate system (r, ϕ, z) both

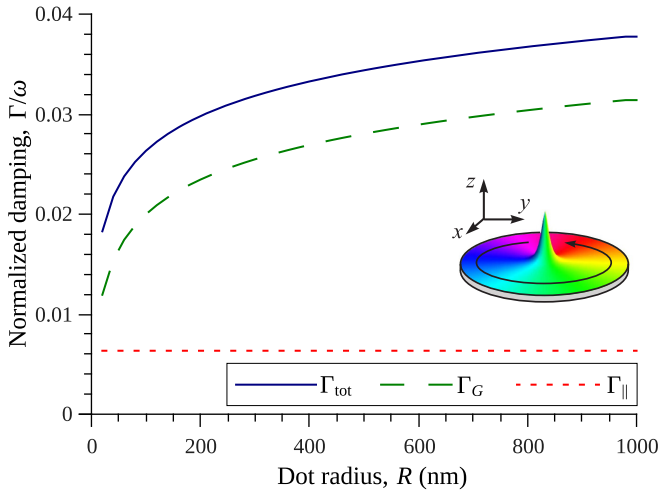

FIG. 1. Normalized damping rate of the gyrotropic mode in a vortex-state circular magnetic dot as a function of the dot radius: Γ_G is the Gilbert damping contribution, $\Gamma_\parallel$ is the contribution from the longitudinal spin diffusion, and $\Gamma_{\rm tot}$ is the total damping rate. The dot material parameters (permalloy) are the exchange length $\lambda_{\rm ex} = 5.5$ nm, $\alpha_G = 0.01$, and the constant of longitudinal spin diffusion [42] $\eta_\parallel = 0.5$ nm^2. The dot thickness is $L = 10$ nm, and the dependence of the vortex core radius on the dot radius and thickness is calculated according to Ref. [44]. (Inset) Circular magnetic nanodot in the vortex state. The spike in the dot center is the vortex core with the polarity $p = 1$, and the in-plane curling magnetization distribution is marked by different colors (vortex chirality $\chi = 1$).

for the description of vectors and coordinate positions inside the dot (the z axis is directed out of the dot's plane, see Fig. 1). In the case of a dot made from a soft ferromagnetic material (like permalloy) the function $\theta(r)$ can be approximated by the Usov-Peschany ansatz [37]: $\theta(r) = 2\arctan[r/b]$ for $r \leqslant b$ and $\theta(r) = \pi/2$ for $r > b$. Here, b is the radius of the vortex core, which is determined by the competition between the exchange and magnetostatic interactions in the dot [38,39], and is of the order of several exchange lengths of the dot's material.

The spectrum of excitations of a vortex-state dot consists of one gyrotropic mode and a set of magnetostatic modes. The gyrotropic, or translational, mode describes the rotation of the vortex core around its equilibrium position (the dot center in the case of a zero bias magnetic field). This mode is the most interesting for our calculation, since in the out-of-core area the magnetization does not precess, but, instead, is oscillating along the linear trajectory in the $\boldsymbol{e}_r$ direction. Therefore, locally, the precession ellipticity is maximal $\mathcal{E} = 1$, leading to a high averaged precession ellipticity of the SW mode, which should lead to a substantial increase of the damping rate of the gyrotropic mode. In the simplest "rigid vortex" model [39], the profile of the gyrotropic mode can be expressed as [40]

$$\boldsymbol{m}_G = R\left(\frac{\partial \boldsymbol{\mu}(\boldsymbol{r}, \boldsymbol{X})}{\partial X} + i\frac{\partial \boldsymbol{\mu}(\boldsymbol{r}, \boldsymbol{X})}{\partial Y}\right)\Bigg|_{\boldsymbol{X}=0}, \tag{4.7}$$

where $\boldsymbol{X} = (X, Y)$ is the two-dimensional vector characterizing the position of the vortex core inside the dot, and R is the dot radius. In terms of the magnetization components in a polar coordinate system, the spatial profile of the gyrotropic mode is given by the expression

$$\boldsymbol{m}_G = Re^{-i\phi}\left(-\frac{i}{r}\sin\theta, \frac{d\theta}{dr}\cos\theta, -\frac{d\theta}{dr}\sin\theta\right). \tag{4.8}$$

Using the explicit expression for the gyrotropic mode profile and Eq. (2.3), one can easily calculate the mode's normalization constant to get $A = 4\pi R^2$. The averaged mode power can also be easily calculated to give $\langle|\boldsymbol{m}_G|^2\rangle = 2\pi R^2(2 + \ln[R/b])$. Thus, according to Eq. (3.9), the effective "ellipticity" coefficient for the gyrotropic mode can be evaluated as

$$\epsilon_G = 1 + \frac{1}{2}\ln\frac{R}{b}. \tag{4.9}$$

This expression has been previously derived in Ref. [7]. One can see, that the above presented general formalism allows one to easily reproduce this result, although the magnetization state of the considered magnetic sample is substantially nonuniform. The dependence of the gyrotropic mode damping rate on the dot radius is shown in Fig. 1 for a permalloy dot. It is clear that for a dot with a radius above 100–200 nm, this damping rate is substantially (2–3 times) larger than the value $\alpha_G\omega$ (result ignoring the mode ellipticity), which is a consequence of the increase of the averaged precession ellipticity of a gyrotropic mode taking place with the increase of a dot radius.

V. SPIN-WAVE DAMPING IN THE PRESENCE OF SPIN DIFFUSION

An important additional mechanism which affects the magnetization dynamics in conducting ferromagnets is the spin diffusion. The time variation of the magnetization in a conducting ferromagnet generates a flow of conduction electrons. The scattering of these electrons on the crystal lattice of a magnetic material contributes to the common Gilbert damping, which is described by the constant α_G. However, if the magnetization dynamics is spatially nonuniform, the flows of conduction electrons generated in different locations inside the ferromagnet become different, leading to the formation of a spin current. This spin current transfers the angular momentum from one point of a ferromagnet to another, thus, influencing the magnetization dynamics. It has been shown recently that this action of the spin current results in an additional damping torque acting on the dynamics of the magnetization [13,41,42].

A. Longitudinal spin diffusion

The spin diffusion is commonly considered to be composed of the longitudinal spin diffusion and the transverse spin diffusion, depending on which component of the spin angular momentum (parallel or perpendicular to the static magnetization, respectively) is transferred by the spin current.

The longitudinal spin diffusion is important for linear magnetization dynamics only in ferromagnets with a nonuniform spatial distribution of the static magnetization. Indeed, in the case of a uniformly magnetized ferromagnet, the excitation of an SW mode produces only a small (of the second order of smallness relative to the mode amplitude) variation of the longitudinal component of magnetization, and, therefore, the

effects of the longitudinal spin diffusion in this case are rather small. The influence of the longitudinal spin diffusion can be described by the term (3.2), where the tensor $\hat{\boldsymbol{D}}_{ad}$ is given by the expression [42]

$$\hat{\boldsymbol{D}}_{ad} = \eta_{\parallel} \sum_{i=x,y,z} \left(\boldsymbol{\mu} \times \frac{\partial \boldsymbol{\mu}}{\partial x_i} \right) \otimes \left(\boldsymbol{\mu} \times \frac{\partial \boldsymbol{\mu}}{\partial x_i} \right). \tag{5.1}$$

Here, $\boldsymbol{\mu} = \boldsymbol{M}(\boldsymbol{r})/M_s$, as defined above, is the distribution of the dimensionless static magnetization, the symbol $\otimes$ denotes the dyadic product of vectors, and the efficiency of the longitudinal spin diffusion is given by the coefficient

$$\eta_{\parallel} = \frac{\gamma \sigma_{\parallel}}{M_s}, \quad \sigma_{\parallel} = \frac{\hbar^2 G_0}{4e^2}, \tag{5.2}$$

where $\sigma_{\parallel}$ is the longitudinal spin conductivity and G_0 is the common electric conductivity of a ferromagnetic metal.

Using Eq. (5.1) in Eq. (3.11), one can easily calculate the enhancement of the damping constant of a SW mode produced by the longitudinal spin diffusion. A typical value of the coefficient $\eta_{\parallel}$, for instance, for permalloy, is $\eta_{\parallel} \sim 0.5$ nm^2. Noting that the common uniform Gilbert damping constant in permalloy is about $\alpha_G \approx 0.01$, it becomes clear that the longitudinal spin diffusion can become an important damping mechanism only if the characteristic length of the considered magnetization texture is less than 10–20 nm. However, the exact value of the enhanced Gilbert constant $\Delta\alpha_G$ could substantially vary for different SW modes, even for the same magnetization texture, and the difference in the magnitude of $\Delta\alpha_G$ in the case of different magnetization textures with similar characteristic lengths could also be significant. That becomes clear if one looks at the complex structure of the tensor $\hat{\boldsymbol{D}}_{ad}$, Eq. (5.1) (see also the example presented below).

B. Transverse spin diffusion

In a uniformly magnetized ferromagnet, instead of the longitudinal spin diffusion, the transverse spin diffusion could play an important role in the damping of the linear magnetization dynamics. Naturally, a transverse spin transfer appears only in the case of a spatially nonuniform *dynamic* magnetization texture, i.e., when the spatially nonuniform SW modes are excited. The influence of the transverse spin diffusion on the magnetization dynamics is described by the term (3.2), where the tensor is defined by the expression [11]

$$\hat{\boldsymbol{D}}_{\perp} = -\eta_{\perp} \nabla^2 \hat{\boldsymbol{I}}, \quad \eta_{\perp} = \frac{\gamma \sigma_{\perp}}{M_s}. \tag{5.3}$$

Here, $\sigma_{\perp}$ is the transverse spin conductivity, which, in a general case, could differ significantly from $\sigma_{\parallel}$, and is not directly related to the electric conductivity of a ferromagnetic metal (see Ref. [11] for details).

Using Eq. (5.3), we arrive to the following expression for the enhanced Gilbert damping constant:

$$\Delta\alpha_G = -\eta_{\perp} \frac{\langle \boldsymbol{m}^* \cdot \nabla^2 \boldsymbol{m} \rangle}{\langle \boldsymbol{m}^* \cdot \boldsymbol{m} \rangle}. \tag{5.4}$$

For SW modes in a bulk ferromagnet, the transverse spin diffusion leads to the additional k^2-dependent damping term, $\alpha_{G,\mathrm{tot}} = \alpha_G + \eta_{\parallel} k^2$. Similarly, for volume SW modes of a magnetic nanoelement, the transverse spin diffusion leads to the damping increase $\alpha_{G,\mathrm{tot}} = \alpha_G + \eta_{\parallel} \kappa^2$, where $\kappa \sim n/w$ is the effective wave number of an SW mode, n is the quantization number of a mode, and w is the characteristic size of a nanoelement (i.e., radius, width, height, etc., depending on the mode structure). As a result, the damping rate of the spatially nonuniform higher-order SW modes is larger than for a quasiuniform one. This, in particular, leads to a suppression of the higher-order SW modes in the ferromagnetic resonance studies [21,24].

It is also clear that the damping increase for bulk SW modes is more pronounced in the case of smaller magnetic nanoelements. For an edge mode, however, as it has been shown in Ref. [18], the dependence $\Delta\alpha_G(w)$ could be opposite, due to the increase in the edge mode localization length with the decrease of the nanoelement size. Since the localization length of the edge mode can be, also, controlled by an external magnetic field, the measurement of the edge mode damping as a function of the external magnetic field could be used to probe the transverse spin conductance and to determine the additional mode damping caused by the transverse spin diffusion.

In bulk ferromagnetic metals, the transverse spin conductance is, typically, smaller than the longitudinal one [11,42]. In thin ferromagnetic films (10 nm thickness) the indirectly measured value of $\sigma_{\perp}$ was found to be similar to the value of the longitudinal spin conductance [18]. Therefore the effect of the transverse spin diffusion on the SW damping will be pronounced only for the sufficiently short-wavelength SW modes, having wavelengths of the order of several tens of nanometers (for permalloy). Note that the transverse spin diffusion takes place, also, in the case of a nonuniform static magnetization distribution inside a ferromagnet. However, to the best of our knowledge, now it is unclear how the corresponding torque term in the Landau-Lifshitz equation should be derived in such a general case. Typically, when the characteristic lengths of the static and dynamic magnetization textures are similar, only the longitudinal spin diffusion is taken into account [42,43].

C. Example: additional damping of spin-wave excitations of a vortex state magnetic nanodot

As another example, we consider the additional damping caused by the longitudinal spin diffusion for an SW mode of a magnetic dot existing in a vortex state. As it was pointed out earlier, the vortex state is highly spatially nonuniform, and the characteristic length of its nonuniformity (the radius of the vortex core) is of the order of several exchange lengths of the dot magnetic material. Therefore one may expect a significant influence of the longitudinal spin diffusion on the damping of the SW modes in this case.

Using the expression for the magnetization distribution (4.6) and the definition of a damping tensor, Eq. (5.1), one can directly calculate the components of the damping tensor in the case of a vortex-state magnetic dot:

$$\hat{\boldsymbol{D}}_{\parallel} = \frac{1}{r^2} \begin{pmatrix} (r d\theta/dr)^2 & 0 & 0 \\ 0 & \sin^2\theta \cos^2\theta & -\cos\theta \sin^3\theta \\ 0 & -\cos\theta \sin^3\theta & \sin^4\theta \end{pmatrix}. \tag{5.5}$$

Here, $\hat{\boldsymbol{D}}_{\parallel}$ is derived in the polar components (i.e., its components are D_{rr}, $D_{r\phi}$, D_{rz}, etc.), and the values of the vortex polarity $p = 1$ and chirality $\chi = 1$ are used below for definiteness. Using this expression and the analytical expression for the profile of gyrotropic SW mode, Eq. (4.8), one finds that $(\boldsymbol{m}_G^* \cdot \hat{\boldsymbol{D}}_{\parallel} \cdot \boldsymbol{m}_G) = 2R^2(d\theta/dr)^2 \sin^2\theta/r^2$. After averaging, the additional damping rate of a gyrotropic mode caused by the spin diffusion is expressed as

$$\Gamma_{\parallel} = \frac{7}{3}\frac{\eta_{\parallel}}{b^2}\omega\,. \tag{5.6}$$

The effective increase of the Gilbert damping constant in this case is, then, equal to

$$\Delta\alpha_G = \frac{14}{3}\frac{\eta_{\parallel}}{b^2(2+\ln[R/b])}\,. \tag{5.7}$$

This expression has been previously derived in a more complex way, starting from the Landau-Lifshitz equation, in Ref. [22].

The radius of the vortex core is almost independent of the dot radius, and increases with the increase of the dot thickness L as $b \approx \lambda_{\rm ex}(2.08 + 0.25(L/\lambda_{\rm ex})^{0.85})$, where $\lambda_{\rm ex}$ is the material exchange length (≈5.5 nm for permalloy) [44]. Noting this dependence, it becomes clear that the damping enhancement for a gyrotropic mode is more pronounced in thinner magnetic dots. Also, due to the increase of the Gilbert damping rate, the relative effect of the spin-diffusion contribution to the total damping becomes smaller with an increase of the dot radius. As shown in Fig. 1, for a 10-nm-thick permalloy dots of radius $R = 100$–200 nm, the contribution of the spin diffusion to the gyrotropic mode damping rate reaches 20%–25%, which, of course, should be taken into account for the proper description of the vortex core dynamics. Spin diffusion is also important for a nonlinear vortex motion, as it has been pointed out in Ref. [43].

In contrast to the gyrotropic mode, all the other excitations of the vortex ground state—magnetostatic modes—are located outside the core region (see modes profiles, e.g., in Refs. [39,45]). Although outside the vortex core, the damping tensor is nonzero due to a curling in-plane magnetization [$D_{\parallel}^{(zz)} \neq 0$, see Eq. (5.5)], our calculations have shown that the longitudinal spin diffusion leads to a negligible damping enhancement, $\Delta\alpha_G < 10^{-3}$ even for a 50-nm dot radius. A rough estimation of the impact of the transverse spin diffusion using Eq. (5.4) (which, as pointed out above, is not rigorously applicable to the case of a nonuniform static magnetization distribution) has shown that this impact for the lowest magnetostatic modes is also negligible. Only if the characteristic wavelength of a magnetostatic mode becomes smaller than 10–20 nm (for permalloy) the transverse spin diffusion starts to be an important channel of the SW mode energy dissipation. Such a case may take place in thicker nanodots (above 40–50 nm in thickness), where the higher-order gyrotropic modes [46], and specific "curled" magnetostaic modes [47] appear, both having spatially nonuniform profiles along the dot thickness. The consideration of this case, however, lies beyond the scope of our current work.

VI. INFLUENCE OF THE INTERLAYER SPIN-PUMPING ON THE DAMPING RATE OF SPIN-WAVE MODES

In the previous section, we considered the case when the spin current, generated by magnetization dynamics, transfers the angular momentum within the ferromagnetic material. However, if a ferromagnet is in contact with another conducting material, the spin current can flow outside of the ferromagnet, or it can be generated in a ferromagnetic-nonmagnetic metal interface, if the ferromagnet is nonconducting. This transfer of angular momentum from a ferromagnet into an adjacent material is called the interlayer spin pumping [48,49].

The spin pumping plays an important role in the magnetization dynamics of ferromagnetic multilayers and heterostructures. In particular, in the case of several conducting ferromagnetic layers separated by ultrathin nonmagnetic spacers, the spin pumping leads to an additional coupling between the ferromagnetic layers [48,50]. If a ferromagnet is in contact with a nonmagnetic metal layer of a sufficient thickness (larger than the spin diffusion length), the spin current generated by time-varying magnetization in a ferromagnetic layer is simply absorbed in the nonmagnetic metal. Naturally, this leakage of the angular momentum plays a role of an additional damping channel for the magnetization dynamics in the ferromagnet [9,10].

The influence of the interlayer spin pumping on the magnetization dynamics is described by the term (3.2) with the damping tensor given by [19]

$$\hat{\boldsymbol{D}} = \eta_s \hat{\boldsymbol{I}}\delta(s(\boldsymbol{r}))\,, \quad \eta_s = \frac{\gamma\hbar^2}{2e^2 M_s} g_{\perp}\,. \tag{6.1}$$

Here, $g_{\perp}$ is the transverse "spin-mixing" conductance per unit area of ferromagnetic-nonmagnetic metal (FM-NM) interface, $\delta(s)$ is the Dirac delta function and the function $s(\boldsymbol{r})$ determines the position of the FM-NM interface. Thus, the expression $\delta(s(\boldsymbol{r}))$ in the equation above means that the interlayer spin pumping affects the magnetization dynamics only at the FM-NM interface. Note that the interlayer spin pumping takes place both in the case of conducting ferromagnets [9,10] and in the case of ferromagnetic insulators [17,19,20]. Equation (6.1) is applicable in both cases if the thickness of the NM layer is larger than the spin diffusion length (which varies from several nanometers up to hundreds of nanometers, depending on the material), and if the conductance of the NM layer is larger than the conductance of the ferromagnetic material.

In the opposite case, which is rather uncommon, one should take into account the effect of the spin accumulation and the back flow of the spin current into the ferromagnetic layer [48]. This, however, cannot be done by a simple modification of Eq. (6.1).

Using the general expression (3.11), we obtain that the enhancement of the damping constant produced by the interlayer spin pumping is equal to

$$\Delta\alpha_G = \eta_s \frac{S}{V}\frac{\langle|\boldsymbol{m}(\boldsymbol{r})|^2\rangle_S}{\langle|\boldsymbol{m}(\boldsymbol{r})|^2\rangle_V}\,, \tag{6.2}$$

where symbols $\langle\ldots\rangle_V$ and $\langle\ldots\rangle_S$ denote the averaging over the volume V of the ferromagnet and over the FM-NM interface, respectively, while S is the area of FM-NM interface. As

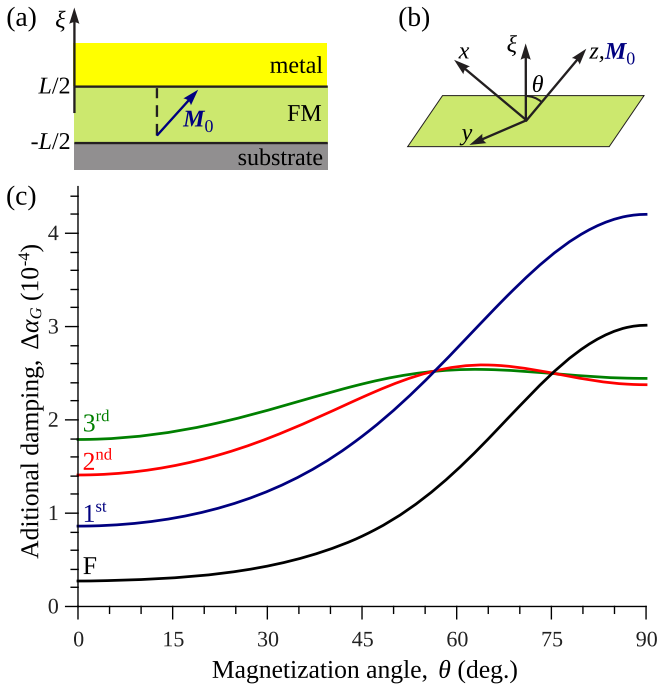

FIG. 2. Spin-pumping-related enhancement of the damping of spin wave modes in an obliquely magnetized magnetic film: (a) sketch of a ferromagnetic film (FM) having the static magnetization $\boldsymbol{M}_0$ and thickness L contacting with a layer of a normal metal; (b) used coordinate system; (c) dependence of the additional damping caused by the interlayer spin pumping on the magnetization angle θ. Calculation parameters: YIG film of thickness 200 nm in contact with gold (Au) and external bias field $B_e = 0.2$ T. Calculations of the thickness profiles of the SW modes were made according to Ref. [51] in the long-wave limit.

one could expect, the enhancement of the damping constant is proportional to the ratio of the oscillation power $|\boldsymbol{m}|^2$ of an SW mode at the interface to the total mode power.

As an example, let us now consider the damping of SW modes in a ferromagnetic film of thickness L, covered at one side by a nonmagnetic metal layer [see Fig. 2(a)]. SW modes propagating in a ferromagnetic film are plane waves with the in-plane wave vector $\boldsymbol{k}$, and a transverse profile along the film thickness described by $\boldsymbol{m}_\nu(\xi)$. In this case, Eq. (6.2) for the damping rate enhancement is reduced to

$$\Delta\alpha_G = \frac{\eta_s}{L}\frac{|\boldsymbol{m}(\xi = L/2)|^2}{\langle|\boldsymbol{m}(\xi)|^2\rangle_\xi}, \tag{6.3}$$

where in the denominator the averaging goes only over the film thickness. The above presented equation is general, and using this equation one can calculate numerically $\Delta\alpha_G$, provided the spatial profiles of the SW modes are known. In several particular cases, the mode profiles $\boldsymbol{m}(\xi)$ could be derived explicitly, which allows one to obtain analytical expressions for the enhanced damping parameters.

In particular, in the case of a negligible surface magnetic anisotropy $K_s \to 0$, which results in the "free" boundary conditions for the dynamic magnetization at the film boundaries, in the long-wave limit ($kL \ll 1$) the profiles of SW modes are given by simple harmonic functions [51]: $\boldsymbol{m}(\xi) = \boldsymbol{m}_n \cos[\pi n(\xi + L/2)]$, $n \in \mathbb{Z}$. Noting that the averaged value $\langle|\boldsymbol{m}(\xi)|^2\rangle = |\boldsymbol{m}_0|^2$ for the uniform mode ($n = 0$) and $\langle|\boldsymbol{m}(\xi)|^2\rangle = |\boldsymbol{m}_n|^2/2$ for all the other modes, one obtains the following expressions for the mode damping enhancements:

$$\Delta\alpha_G = \frac{\eta_s}{L} \text{ for } n = 0\,, \quad \Delta\alpha_G = 2\frac{\eta_s}{L} \text{ for } n \neq 0\,. \tag{6.4}$$

In a more complex way this result has been obtained previously in Ref. [19].

In the case of a nonzero surface anisotropy, the amplitude of the volume SW modes at the film boundary becomes smaller and, naturally, in that case the spin-pumping into the adjacent metallic layer leads to a smaller enhancement of the damping rate. The only exception from this rule is the surface mode, which exists if the pinning parameters are negative (for a perpendicularly magnetized film such a case is realized if $K_s < 0$, which means an easy-plane surface anisotropy). Since the surface mode is strongly localized at the surfaces, the interlayer spin-pumping has a much stronger effect on this surface mode. In the case of a relatively strong surface pinning, the profile of the surface mode can be approximated as $\boldsymbol{m} \sim \exp[Q(\xi - L/2)]$ (mode is localized at the $\xi = L/2$ surface), which leads to a thickness-independent enhanced of the mode damping rate:

$$\Delta\alpha_G = 2\eta_s\frac{|K_s|}{A}, \tag{6.5}$$

where $Q = |K_s|/A$ is the inverse localization length of the surface mode. Naturally, the other surface mode, localized at the opposite surface of the film [$\xi = -L/2$ in Fig. 2(a)], where the nonmagnetic metal layer is absent, experiences a negligible damping enhancement.

The above developed method allows one, also, to analyze a more general case of a nonuniform pinning of dynamical magnetization at the film surfaces, which is realized when the film is magnetized at an arbitrary angle θ to its normal. For instance, we calculated the damping enhancement for SW modes having different thickness profiles and propagating in an yttrium-iron-garnet (YIG) film contacting at one side with a layer of gold (Au). The calculation parameters were the saturation magnetization $\mu_0 M_s = 0.175$ T, the exchange stiffness $A = 3.5 \times 10^{-12}$ J/m, the easy-axis surface anisotropy constant $K_s = 5 \times 10^{-5}$ J/m, and the transverse spin-"mixing" conductance $hg_\perp/e^2 = 1.2 \times 10^{18}$ m^{-2} [52].

The thickness profiles of the SW modes propagating in a magnetic film depend significantly on the magnetization angle. In particular, in the considered case of an easy-axis surface anisotropy, which was assumed to be the same at both interfaces of a ferromagnetic film, in the case of perpendicular magnetization ($\theta = 0$) all the SW modes are volume modes having sinusoidal thickness profiles. However, when the static magnetization tilts toward the in-plane direction ($\theta > 0$), the two lowest thickness SW modes are transformed into surface modes (in general, the number of the surface modes depends on the strength of the surface anisotropy at the film interfaces, and could be zero, one, or two [51]). This transformation is clearly seen in the dependencies of the damping parameter enhancement $\Delta\alpha_G$ on the magnetization angle, which are shown in Fig. 2(c).

For the second, third, and all the higher thickness SW modes, which remain volume modes at all values of the magnetization angle, the dependencies are nonmonotonic, having the maximum at $\theta \approx 50^\circ$–60°. The appearance of this maximum is related to the angular dependence of the pinning parameters for both dynamic magnetization components, $d_x \sim \cos 2\theta$, $d_y \sim \cos^2\theta$, [51] which, finally, results in the almost unpinned mode profiles at the considered magnetization angles. The maximum value of the damping enhancement is close to $\Delta\alpha_G \sim 2\eta_s/L$, which was obtained above for the case of "free" (unpinned) boundary conditions.

In contrast, the angular dependence of the damping enhancement $\Delta\alpha_G(\theta)$ for the lowest (fundamental, F) mode and the first thickness modes shows a monotonous increase with the magnetization angle θ, which is a direct consequence of the angular-dependent transformation of the mode "volume" to "surface," and the consequent increase of the influence of the interlayer spin pumping on the SW mode damping.

Taking into account the fact that the natural Gilbert damping in a YIG film is $\alpha_G \approx (2\text{–}3) \times 10^{-4}$, it becomes clear that for the films of thickness $L \sim 200$ nm and less, the interlayer spin pumping could become an important, or even a dominant, source of the energy dissipation of the SW modes in YIG films.

In comparison, for the other widely used magnetic material, permalloy, the spin-mixing conductance is of the order of $hg_\perp/e^2 = 10^{19}$ m^{-2} (for Py-Cu [10] and Py-Ta [18] interfaces), but due to the higher saturation magnetization of the permalloy [$\eta_s \sim 1/M_s$, see Eq. (6.1)] and the higher intrinsic Gilbert damping ($\alpha_G \sim 0.005$–0.01), the influence of the interlayer spin pumping becomes significant only for very thin films, having thicknesses less than 10 nm, or for a surface SW mode having a similar localization depth.

Finally, we would like to note that the dependencies $\Delta\alpha_G(\theta)$ shown in Fig. 2(c) with the maxima at $\theta \approx 50^\circ$–60° for all the SW modes except the one or two surface modes [51] provide a clear signature of the fact that the additional SW damping is caused by the interlayer spin pumping. Therefore such dependencies could be used to experimentally identify the cases when spin pumping provides an important additional damping channel for SW modes.

VII. CONCLUSIONS

In this work, we developed a general theoretical approach to describe the damping of spin-wave modes of ferromagnetic samples and nanostructures in the presence of different *linear* damping mechanisms, which could be spatially nonuniform or dependent on the magnetization texture (nonlocal). In the case of a relatively small magnetic damping, i.e., if the damping rate of an SW mode is significantly smaller than the mode eigenfrequency, the SW damping rates could be successfully calculated in the framework of a perturbation theory. Using this perturbative approach, we derive a simple expression for the damping rate of an SW mode having an arbitrary spatial profile.

Using the developed formalism, we have shown that the SW damping rate due to the common Gilbert damping is directly related to the SW dispersion relation, namely, is determined by the variational derivative of the dispersion relation by the internal static magnetic field. In other words, it could be stated that the SW mode damping rate is related to the averaged precession ellipticity, and it increases when the ellipticity becomes larger. For this reason, for example, the gyrotropic mode of a vortex-state magnetic dot has a significantly larger damping rate than a fundamental SW mode in a uniformly magnetized magnetic film $\alpha_G\omega$, because the gyrotropic mode has an almost linear polarization (maximum ellipticity) away from the area of the vortex core.

To illustrate the power of the developed theoretical approach, we considered the influence of spin diffusion and interlayer spin-pumping on the damping rate of SW modes. In particular, it was shown that the longitudinal spin diffusion can substantially increase the damping rate of the gyrotropic mode of the vortex-state magnetic nanodot. In contrast, the magnetostatic modes of a vortex-state nanodot are practically unaffected by these dissipation mechanisms, as long as their characteristic wavelength is larger than 10–20 nm (for permalloy).

In the case of the interlayer spin pumping, the enhancement of the SW mode damping rate is proportional to the ratio of the SW mode oscillation power $|\boldsymbol{m}|^2$ at the interface to the total power of the SW mode, and, naturally, the surface modes are the modes that are strongly affected by the spin pumping.

In a ferromagnetic film placed in contact with a layer of a normal metal, the dependence of the effective pinning parameters and, consequently, the SW mode thickness profiles, on the magnetization angle θ leads to a complex dependence of the damping constant enhancement on the magnetization angle θ. The characteristic features of the dependence $\Delta\alpha_G(\theta)$—the existence of a local maximum at $\theta \approx 50^\circ$–60° for all the SW modes except one or two surface modes—could be used to experimentally detect the situations when the interlayer spin pumping has a significant influence on the magnetization dynamics.

ACKNOWLEDGMENTS

This work was supported by the Grants No. EFMA-1641989 and No. ECCS-1708982 from the NSF of the USA, and by the DARPA M3IC Grant under the Contract No. W911-17-C-0031. R.V. acknowledges support from the Ministry of Education and Science of Ukraine (Projects No. 0115U002716 and No. 0118U004007).

[1] *Advanced Magnetic Nanostructures*, edited by D. J. Sellmyer and R. Skomski (Springer, New York, 2006).

[2] A. G. Gurevich and G. A. Melkov, *Magnetization Oscillations and Waves* (CRC Press, New York, 1996).

[3] A. Slavin and V. Tiberkevich, IEEE Trans. Magn. **45**, 1875 (2009).

[4] M. Sparks, *Ferromagnetic Relaxation Theory* (McGraw-Hill, New York, 1964).

[5] T. Gilbert, IEEE Trans. Magn. **40**, 3443 (2004).
[6] D. D. Stancil, J. Appl. Phys. **59**, 218 (1986).
[7] K. Y. Guslienko, Appl. Phys. Lett. **89**, 022510 (2006).
[8] V. Tiberkevich and A. Slavin, Phys. Rev. B **75**, 014440 (2007).
[9] Y. Tserkovnyak, A. Brataas, and G. E. W. Bauer, Phys. Rev. Lett. **88**, 117601 (2002).
[10] T. Gerrits, M. L. Schneider, and T. J. Silva, J. Appl. Phys. **99**, 023901 (2006).
[11] Y. Tserkovnyak, E. M. Hankiewicz, and G. Vignale, Phys. Rev. B **79**, 094415 (2009).
[12] K. Gilmore and M. D. Stiles, Phys. Rev. B **79**, 132407 (2009).
[13] C. H. Wong and Y. Tserkovnyak, Phys. Rev. B **80**, 184411 (2009).
[14] C. A. Akosa, I. M. Miron, G. Gaudin, and A. Manchon, Phys. Rev. B **93**, 214429 (2016).
[15] M. L. Schneider, J. M. Shaw, A. B. Kos, T. Gerrits, T. J. Silva, and R. D. McMichael, J. Appl. Phys. **102**, 103909 (2007).
[16] H. T. Nembach, J. M. Shaw, T. J. Silva, W. L. Johnson, S. A. Kim, R. D. McMichael, and P. Kabos, Phys. Rev. B **83**, 094427 (2011).
[17] C. W. Sandweg, Y. Kajiwara, K. Ando, E. Saitoh, and B. Hillebrands, Appl. Phys. Lett. **97**, 252504 (2010).
[18] H. T. Nembach, J. M. Shaw, C. T. Boone, and T. J. Silva, Phys. Rev. Lett. **110**, 117201 (2013).
[19] A. Kapelrud and A. Brataas, Phys. Rev. Lett. **111**, 097602 (2013).
[20] H. Skarsvåg, A. Kapelrud, and A. Brataas, Phys. Rev. B **90**, 094418 (2014).
[21] W. Wang, M. Dvornik, M.-A. Bisotti, D. Chernyshenko, M. Beg, M. Albert, A. Vansteenkiste, B. V. Waeyenberge, A. N. Kuchko, V. V. Kruglyak, and H. Fangohr, Phys. Rev. B **92**, 054430 (2015).
[22] O. V. Sukhostavets, J. M. Gonzalez, and K. Y. Guslienko, Low Temp. Phys. **41**, 772 (2015).
[23] A. Bisig, C. A. Akosa, J.-H. Moon, J. Rhensius, C. Moutafis, A. von Bieren, J. Heidler, G. Kiliani, M. Kammerer, M. Curcic, M. Weigand, T. Tyliszczak, B. Van Waeyenberge, H. Stoll, G. Schütz, K.-J. Lee, A. Manchon, and M. Kläui, Phys. Rev. Lett. **117**, 277203 (2016).
[24] Y. Li and W. E. Bailey, Phys. Rev. Lett. **116**, 117602 (2016).
[25] C. A. Akosa, P. B. Ndiaye, and A. Manchon, Phys. Rev. B **95**, 054434 (2017).
[26] L. Rozsa, J. Hagemeister, E. Y. Vedmedenko, and R. Wiesendanger, arXiv:1805.01815 [Phys. Rev. B (to be published)].
[27] A. Vansteenkiste, J. Leliaert, M. Dvornik, M. Helsen, F. Garcia-Sanchez, and B. Van Waeyenberge, AIP Adv. **4**, 107133 (2014).
[28] L. Lopez-Diaz, D. Aurelio, L. Torres, E. Martinez, M. A. Hernandez-Lopez, J. Gomez, O. Alejos, M. Carpentieri, G. Finocchio, and G. Consolo, J. Phys. D: Appl. Phys. **45**, 323001 (2012).
[29] V. V. Naletov, G. de Loubens, G. Albuquerque, S. Borlenghi, V. Cros, G. Faini, J. Grollier, H. Hurdequint, N. Locatelli, B. Pigeau, A. N. Slavin, V. S. Tiberkevich, C. Ulysse, T. Valet, and O. Klein, Phys. Rev. B **84**, 224423 (2011).
[30] R. Verba, G. Melkov, V. Tiberkevich, and A. Slavin, Phys. Rev. B **85**, 014427 (2012).
[31] R. V. Verba, Ukrainian J. Phys. **58**, 758 (2013).
[32] K.-W. Kim, J.-H. Moon, K.-J. Lee, and H.-W. Lee, Phys. Rev. Lett. **108**, 217202 (2012).
[33] R. Cheng, J.-G. Zhu, and D. Xiao, Phys. Rev. Lett. **117**, 097202 (2016).
[34] K. Ando, S. Takahashi, K. Harii, K. Sasage, J. Ieda, S. Maekawa, and E. Saitoh, Phys. Rev. Lett. **101**, 036601 (2008).
[35] L. Liu, T. Moriyama, D. C. Ralph, and R. A. Buhrman, Phys. Rev. Lett. **106**, 036601 (2011).
[36] A. A. Mailybaev and A. P. Seiranian, *Multiparameter Stability Problems. Theory and Applications in Mechanics* (Fizmatlit, Moskow, 2009) (in Russian).
[37] N. Usov and S. Peschany, J. Magn. Magn. Mater. **118**, L290 (1993).
[38] K. L. Metlov and K. Y. Guslienko, J. Magn. Magn. Matter. **242-245**, 1015 (2002).
[39] K. Y. Guslienko, J. Nanosci. Nanotechnol. **8**, 2745 (2008).
[40] K. Y. Guslienko, A. N. Slavin, V. Tiberkevich, and S.-K. Kim, Phys. Rev. Lett. **101**, 247203 (2008).
[41] J. Foros, A. Brataas, Y. Tserkovnyak, and G. E. W. Bauer, Phys. Rev. B **78**, 140402 (2008).
[42] S. Zhang and S. S.-L. Zhang, Phys. Rev. Lett. **102**, 086601 (2009).
[43] J.-H. Moon and K.-J. Lee, J. Appl. Phys. **111**, 07D120 (2012).
[44] O. V. Sukhostavets, G. R. Aranda, and K. Y. Guslienko, J. Appl. Phys. **111**, 093901 (2012).
[45] B. A. Ivanov and C. E. Zaspel, Phys. Rev. Lett. **94**, 027205 (2005).
[46] J. Ding, G. N. Kakazei, X. Liu, K. Y. Guslienko, and A. O. Adeyeye, Sci. Rep. **4**, 4796 (2014).
[47] R. V. Verba, A. Hierro-Rodriguez, D. Navas, J. Ding, X. M. Liu, A. O. Adeyeye, K. Y. Guslienko, and G. N. Kakazei, Phys. Rev. B **93**, 214437 (2016).
[48] Y. Tserkovnyak, A. Brataas, G. E. W. Bauer, and B. I. Halperin, Rev. Mod. Phys. **77**, 1375 (2005).
[49] A. Brataas, A. D. Kent, and H. Ohno, Nat. Mater. **11**, 372 (2012).
[50] Y. Tserkovnyak, A. Brataas, and G. E. W. Bauer, Phys. Rev. B **67**, 140404 (2003).
[51] B. A. Kalinikos and A. N. Slavin, J. Phys. C: Solid State Phys. **19**, 7013 (1986).
[52] B. Heinrich, C. Burrowes, E. Montoya, B. Kardasz, E. Girt, Y.-Y. Song, Y. Sun, and M. Wu, Phys. Rev. Lett. **107**, 066604 (2011).